

Supplemental Figure Legends

Supplemental Figure 1: Characterization of transcription factory structure and function in cardiomyocytes.

A) 5'Fluorouridine (5'FU) is a uracil analogue that can permeate live cells and be incorporated into synthesizing RNA. Sites of 5'FU incorporation can then be detected using immunofluorescence. Representative image of neonatal rat ventricular myocytes treated with 4mM 5'FU for 30min is shown (*left*). RNase A treatment, post-5'FU incorporation, shows absence of 5'FU signal, demonstrating specificity of labeling to RNA (*right*). *Scale bar: 5 μ m.* **B)** RNA polymerase I activity quenches 5'FU signal into the nucleolus while treatment with CX-5461 allows for selective labeling of transcriptional activity in the nucleoplasm, which is associated with sites of active RNA polymerase II (phosphorylated at serine 2) occupancy, indicated by co-localization (*yellow*). *Scale bar = 5 μ m.* **C)** The distribution of nucleoli number does not differ with hypertrophic stress. **D)** NRVMs were treated with CX-5461, an RNA polymerase I inhibitor (2 μ M, 15min), prior to the addition of 5'FU. Thus, 5'FU labeling is reflective of RNA polymerase II and III activity. Note the absence of signal in the nucleolus, marked by nucleolin. *Scale bar = 5 μ m.* **E)** CX-5461 treatment efficiency in inhibiting RNA polymerase I was confirmed by measuring ribosomal RNA expression, ITS (premature) and 18S (mature) at 15min (before addition of 5'FU) and 45min (time point at which cells were fixed for immunostaining). *15min: n=4; 45min: n=6. Error bars represent SEM.* **F)** NRVMs were treated with 10 μ M phenylephrine for 48hr, after which they were fixed and labeled with phalloidin and DAPI for cell and nuclear size measurements. *Scale bar = 25 μ m.* **G)** Quantifications of cell and nuclear sizes show significant increases in cell (60% increase) and total nuclear (8% increase) areas. The ratio of total nuclear area to cell area was significantly reduced in the hypertrophic cardiomyocytes, highlighting greater growth of the cell versus nucleus (nuclear occupancy is reduced to 8% of the cell from 12%). The increase in nuclear size does not affect nuclear shape, indicated by circularity (a perfect circle has circularity value of 1). *Control: n=259 cells (279 nuclei); Phenylephrine: n=255 cells (279 nuclei).* **H)** Nuclei number after phenylephrine treatment is unaltered. *Control: n=323 cells, Phenylephrine: n=372 cells.* **I)** NRVMs treated with isoproterenol (1 μ M for 48hr) show minimal hypertrophy response. *Scale bar = 25 μ m.* **J)** Phenylephrine treatment induces robust pathological gene expression. **K)** The relationship between mean 5'FU intensity and cell area were compared. There was no significant correlation between nascent transcript levels and cell size (control: $r=0.177$, $p=0.133$; phenylephrine: $r=0.083$, $p=0.515$). *Control: n=73 cells; Phenylephrine: n=64 cells. * $p<0.05$; ** $p<0.001$ [Mann-Whitney; for nucleoli number distribution, Chi-squared].*

Supplemental Figure 2: Super-resolution mapping of cardiac transcription factories.

A) NRVMs treated with phenylephrine were labeled for active RNA polymerase II, phosphorylated at serine 2, and

5'fluorouridine incorporation (2 μ M CX-546, 4mM 5'FU) and imaged with STED microscopy. *Left* image shows the confocal image of a control nucleus with its corresponding super-resolution image on the *right*. Boxed regions highlight the level of detail that can be resolved with the STED microscope. *Scale bar = 2 μ m (1 μ m for magnification).* **B)** Nuclear area increases with hypertrophy in the cells used for these analyses. **C)** RNA polymerase II clusters are mapped and color-coded based on mean cluster intensity. Analyses examining the intensity ranges (measuring the minimum and maximum intensities per nucleus) demonstrate no difference with hypertrophic agonist treatment. *Control: n=10 nuclei; Phenylephrine: n=11 nuclei. Scale bar = 5 μ m.* **D)** Adult cardiomyocyte transcription factories were analyzed *in situ* from heart tissue sections. Cardiac nuclei were distinguished from non-cardiomyocyte nuclei using desmin labeling. *Scale bar = 50 μ m (5 μ m for magnification).* ** $p < 0.001$ [Mann-Whitney].

Supplemental Figure 3: Properties of RNA polymerase II factories in hypertrophic and failing cardiomyocytes.

A) The normalized distance to the nuclear envelope shows no change in neonatal cardiomyocytes (normalized to radial distance to account for differences in nuclear size). **B)** The average of intensity of the top 20% intensity ranked clusters does not differ. When normalizing peripheral distance, there is a decrease in distance from the periphery though not significant. **C)** The positioning across the nucleus of the most intense clusters shows no change in distribution after hypertrophic stress (*left*). Enrichment was determined by comparing fraction of the most intense clusters to the fraction of total clusters for each bin (*right*). **D)** 5'Fluorouridine intensity is significantly reduced in hypertrophic myocytes. **E)** The average spacing between nearest neighboring 5'fluorouridine puncta does not change. **F)** The normalized distance of 5'fluorouridine clusters to the nuclear periphery decreases. **G)** Cluster number was normalized to nuclear area and indicated no difference with pressure overload in adult mouse cardiac nuclei. The nuclei that were analyzed had similar areas. Nucleoplasmic regions were determined based on presence of RNA polymerase II signal. Regions devoid of signal were regions associated with nucleoli or characteristic cardiomyocyte heterochromatin chromocenters. The ratio of nucleoplasm to nuclear area does not change. **H)** Cluster distances to the periphery were normalized to area and are not different between groups. **I)** The mean intensity of the highly ranked clusters significantly increases with TAC stress. The bottom 20%-ranked clusters have increases in mean intensity without changes to spatial organization in the nucleus (distance to nuclear envelope, $p=0.689$). **J)** To normalize nuclear distances, the difference between maximum and minimum distances to the nuclear periphery was used to generate 5 bins. *Scale bar = 3 μ m.* **K)** The top 20% most intense clusters were examined. The distribution of intensity shows that these clusters are found across the nucleus without preferential localization as indicated by the comparable mean intensity at each bin across the nucleus ($p < 0.001$, two-way ANOVA). **L)** Examination of cluster enrichment (fraction of top intense clusters divided by fraction of total clusters

per bin) suggests that there is a reduction in highly intense clusters from the nuclear periphery (*right*). *Sham*: $n=21$ nuclei; *TAC*: $n=20$ nuclei. * $p<0.05$; ** $p<0.001$ [Mann-Whitney; for cluster distribution, Chi-squared]. Error bars represent SEM.

Supplemental Figure 4: Validation of cardiac-specific changes in gene expression. **A)** RNA expression levels of four genes to be further analyzed by DNA FISH are validated in isolated adult cardiomyocytes. These genes were chosen to represent four categories of expression responses due to stress (activation, silencing, remain active and remain silent) and serve as models to understand genomic organization in cardiomyocytes. *Nppa* and *Atp2a2* expression (normalized to *Gapdh*) occur in a cardiac-specific manner; the liver expression is shown for comparison (*i*). *Nefl* expression, a neuronal gene, serves as a negative control in both heart and liver tissues (normalized to *Gapdh* expression) (*ii*). Changes in expression of *Nppa* and *Atp2a2* after TAC are shown (*iii*), along with raw expression of *Gapdh* (*iv*). Error bars represent SEM. **B)** The changes in expression on the level of RNA reflect the changes in protein abundance. Quantifications of western blots are shown on *right*. Molecular weights for ANF ~17kDa, SERCA2 ~110kDa, NEFL ~68kDa, GAPDH ~37kDa.

Supplemental Figure 5: Distribution of DNA FISH loci in liver nuclei is unaffected after pressure-overload stress. DNA FISH labeling in liver tissue from mice with heart failure was used to assess tissue-specificity of genomic architecture. Furthermore, based on DAPI patterns, liver nuclei have different nuclear shape and architecture. The distributions of *Atp2a2* (**A**), *Nppa* (**B**), *Gapdh* (**C**) and *Nefl* (**D**) are not affected by TAC surgery. Quantitation is compiled from different labeling experiments from 2 different mice per treatment. *Atp2a2*: *Sham* $n=78$ nuclei/95 loci, *TAC* $n=107/138$; *Nppa*: *Sham* $n=102/119$, *TAC* $n=102/125$; *Gapdh*: *Sham* $n=98/116$, *TAC* $n=112/119$; *Nefl*: *Sham* $n=99/111$, *TAC* $n=104/122$. Scale bar = 5 μ m. *P* values were calculated using Chi-squared.

Supplemental Figure 6: RNA polymerase II occupancy confirms relationship between gene expression and association with transcription factories. The coordinates of DNA FISH primers were converted from mm10 to mm9 (using liftOver tool) to compare to published RNA polymerase II ChIP-seq (active RNA polymerase II, phosphorylated at serine 2) performed from whole heart lysates of sham and TAC mice (4 days after surgery) [39]. The mapped signal from ChIP-seq (sham in *blue*, TAC in *red*) at the regions targeted by DNA FISH is shown on *left*. Each red bar represents location of 200bp fragments that constitute DNA FISH probe tiling genomic loci; dotted boxes mark gene bodies. Fragment density indicates the number of mapped fragments per bin. ChIP-PCR was performed on isolated cardiomyocytes pooled from 6-7mice/group that were in heart failure (~6 weeks after TAC; *right*). IPs

were normalized to input and fold enrichment over IgG is shown (n=3 technical replicates, data is representative of 4 independent IPs). Locations of the primers used for promoter and gene body regions are indicated by arrows. These results show increased enrichment of RNA polymerase II at the *Nppa* gene body, decreased enrichment at *Atp2a2* and *Gapdh* genes and no enrichment at the *Nefl* gene. *Error bars represent SEM. P values were calculated using two-tailed t-test.*

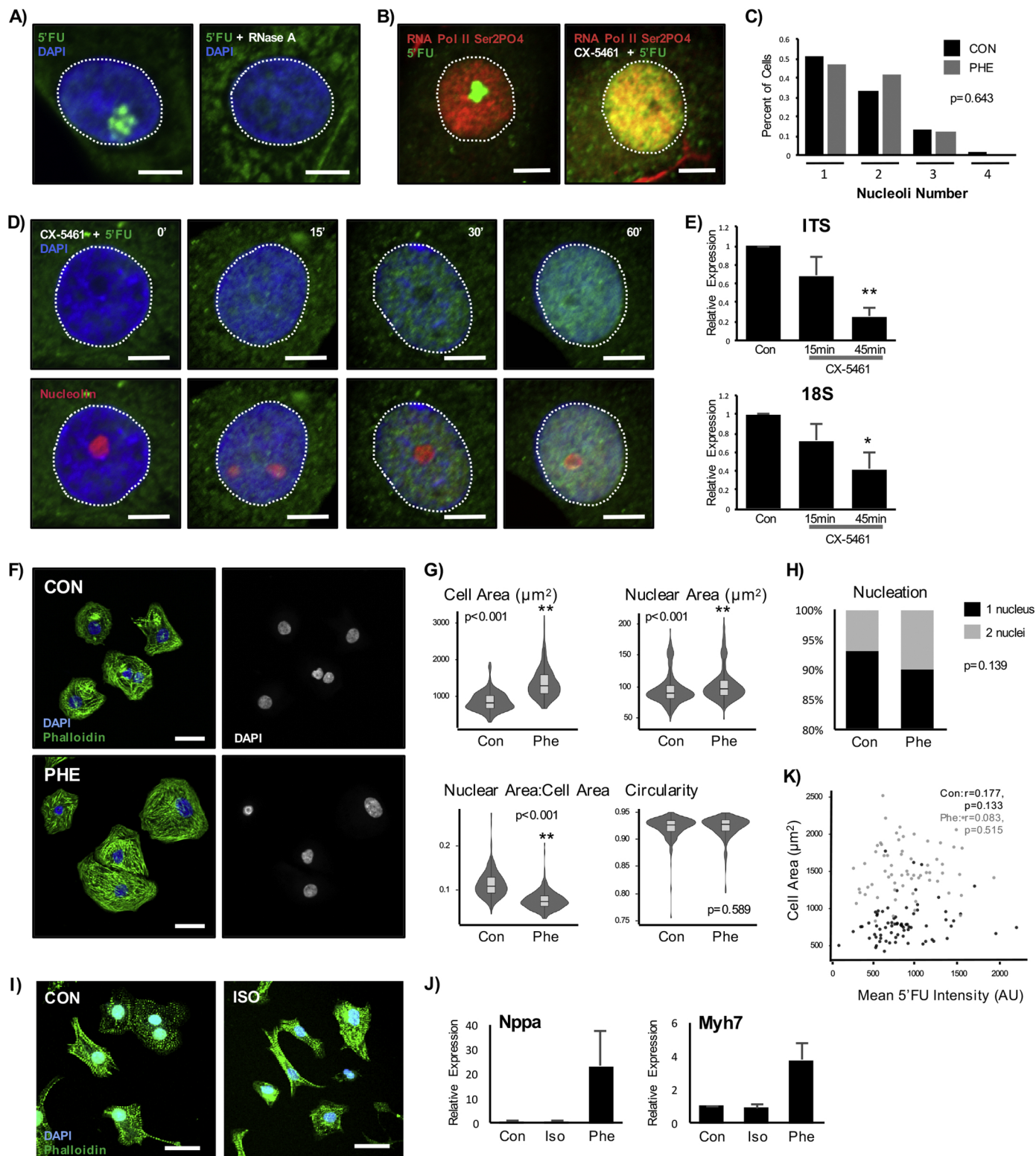


Figure 7

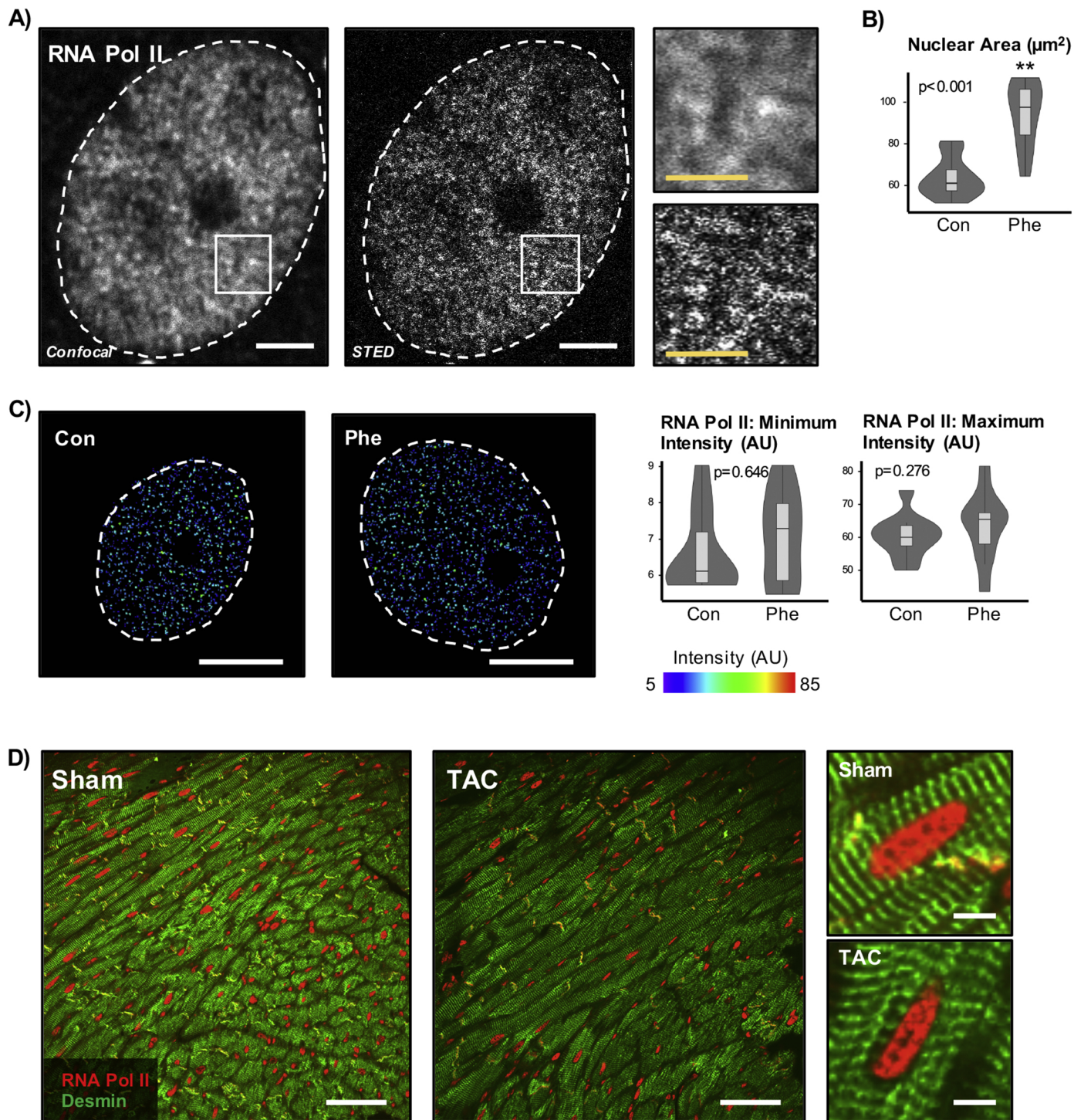
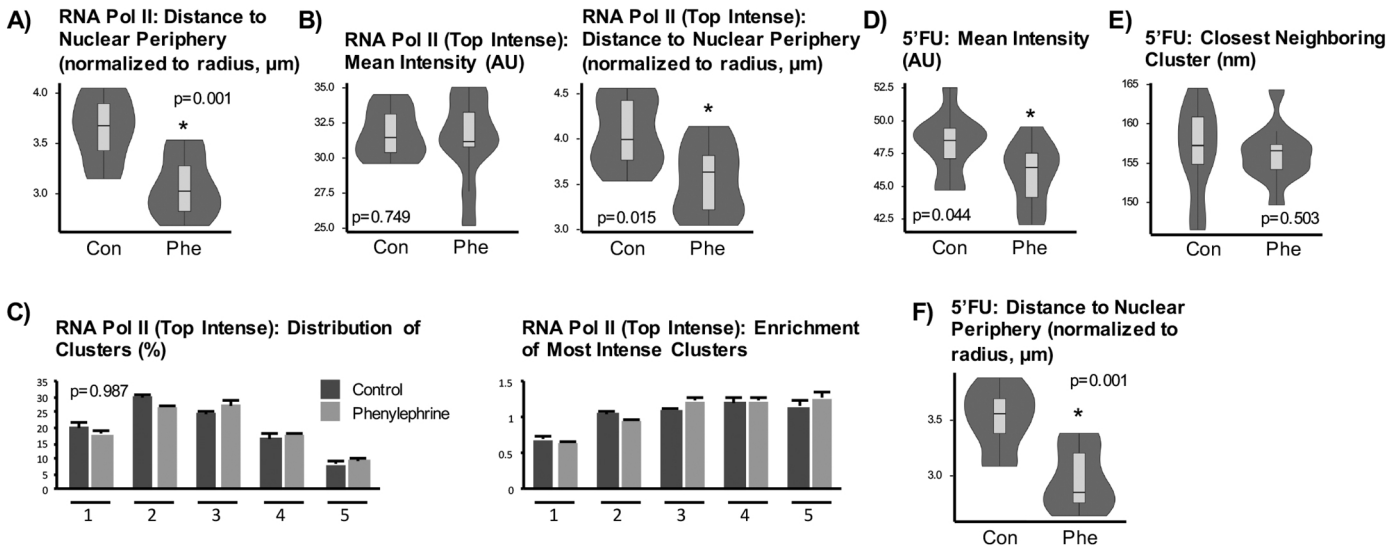


Figure 8

Neonatal Rat Cardiomyocytes



Adult Mouse Heart Tissue (Cardiomyocytes)

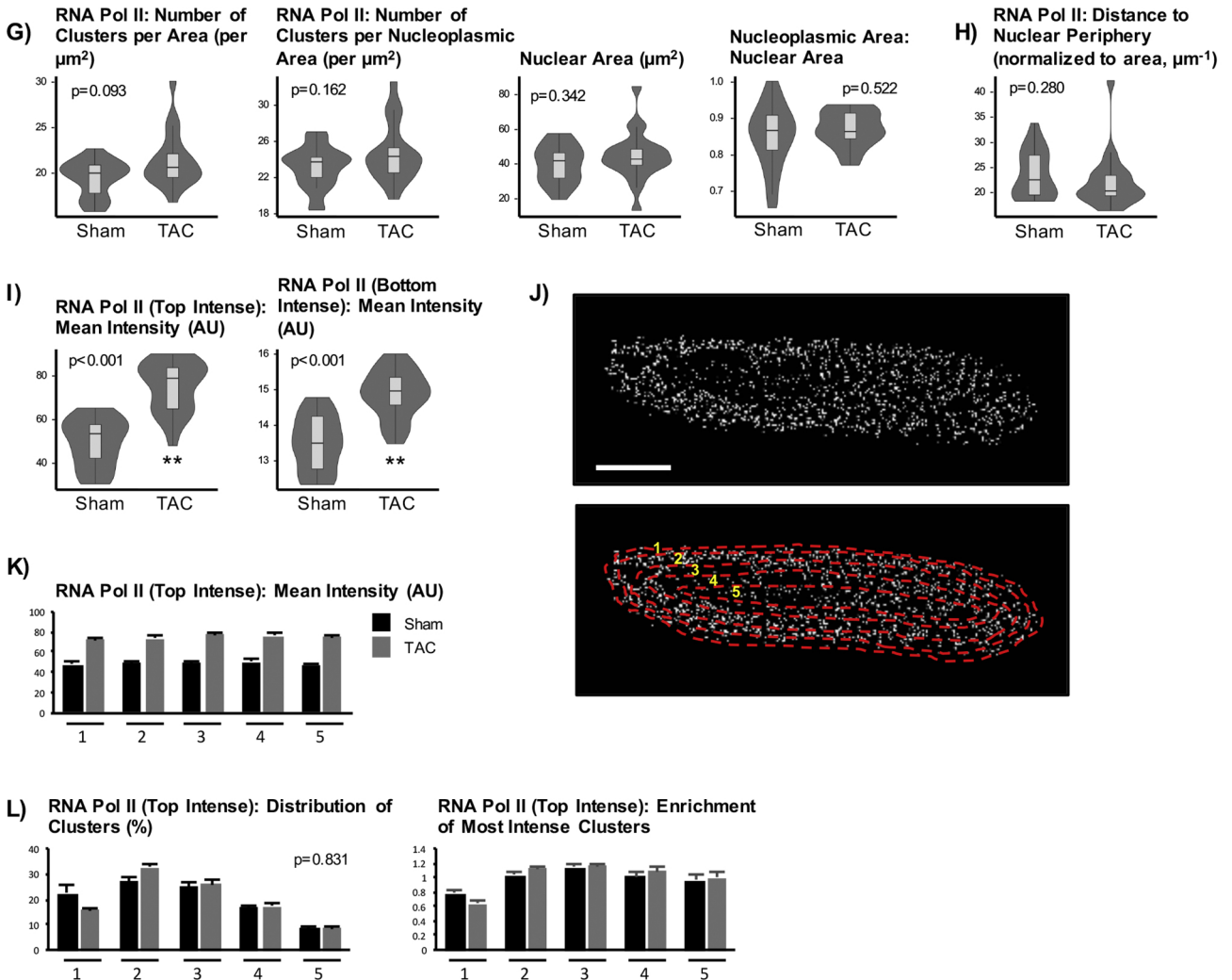
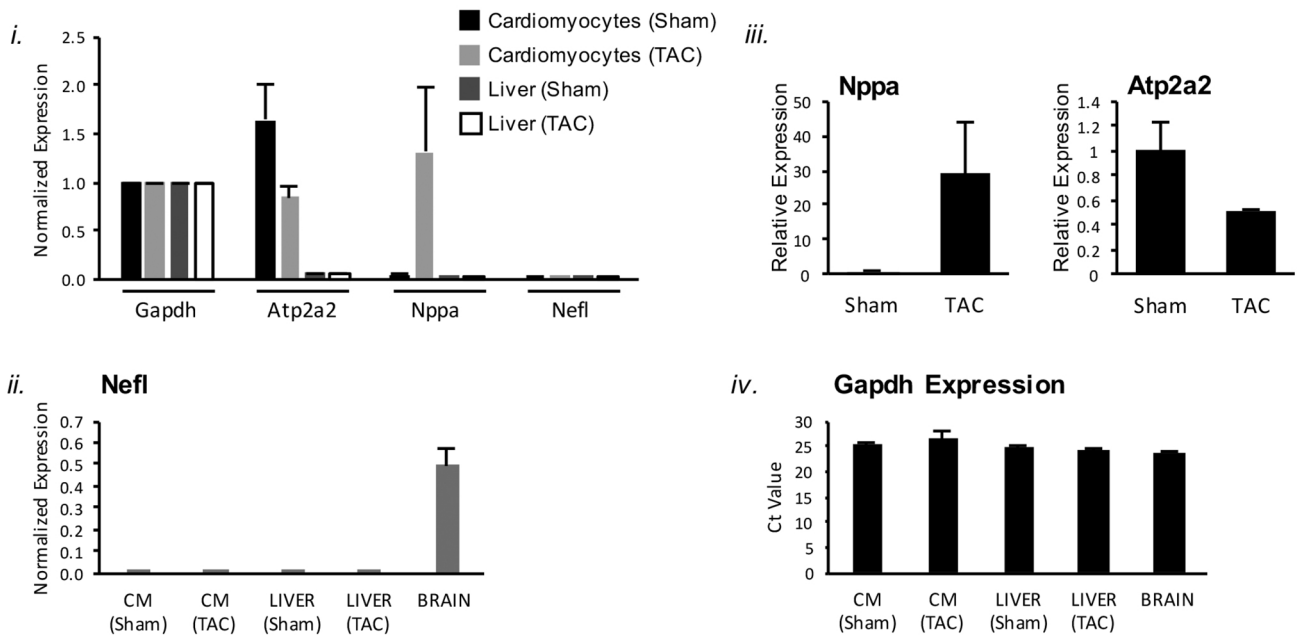


Figure 9

A) RNA Expression:



B) Protein Expression:

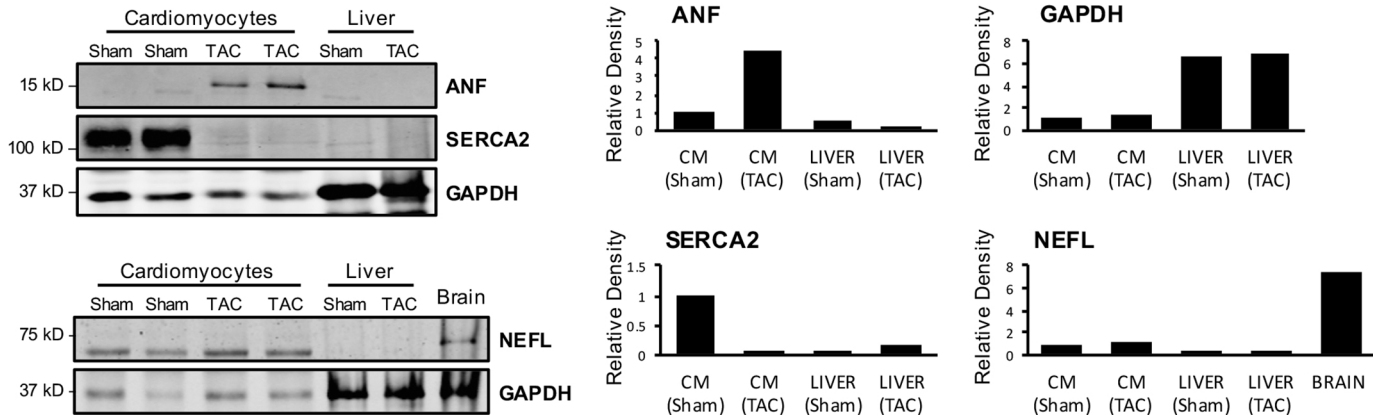


Figure 10

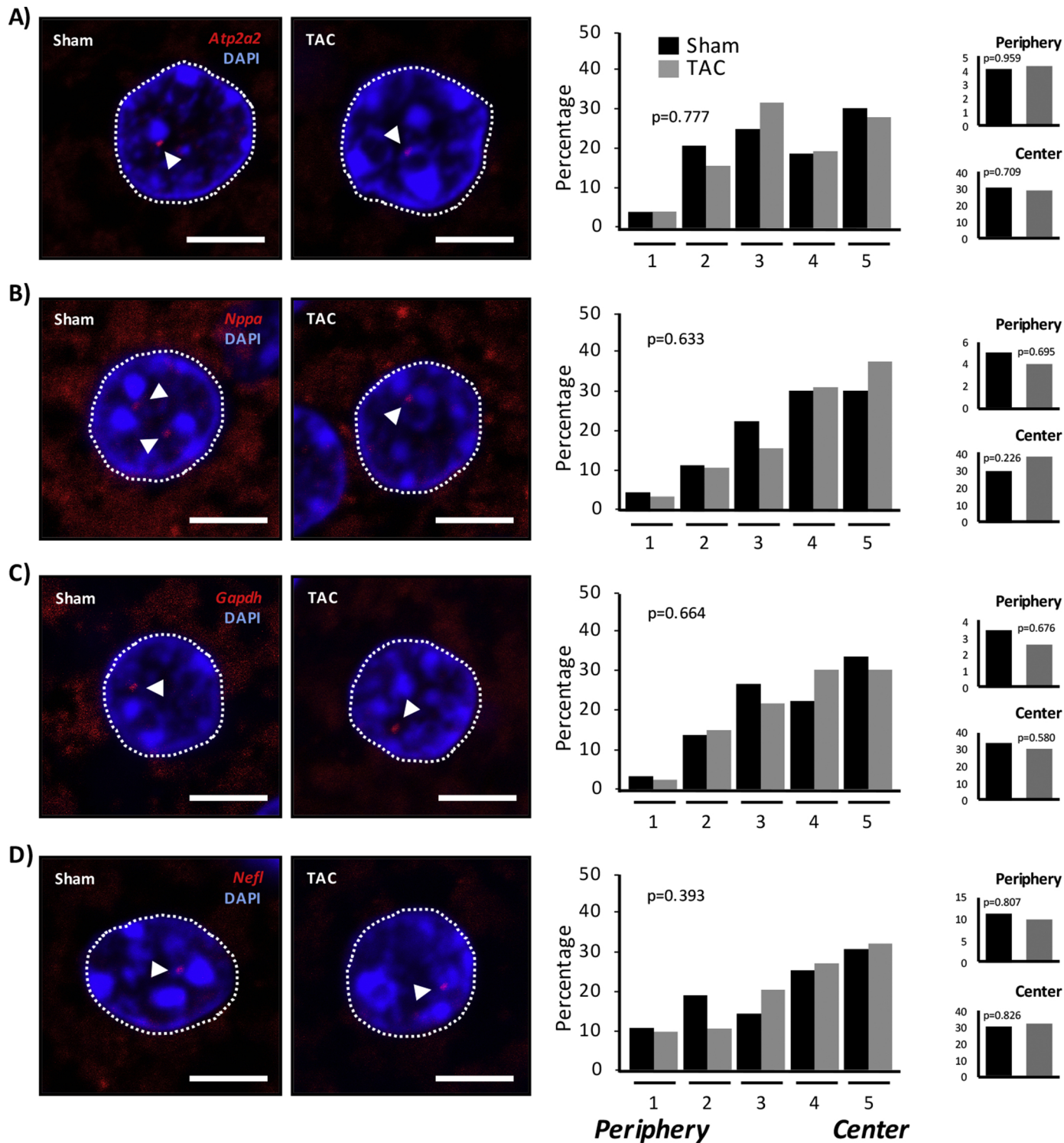


Figure 11

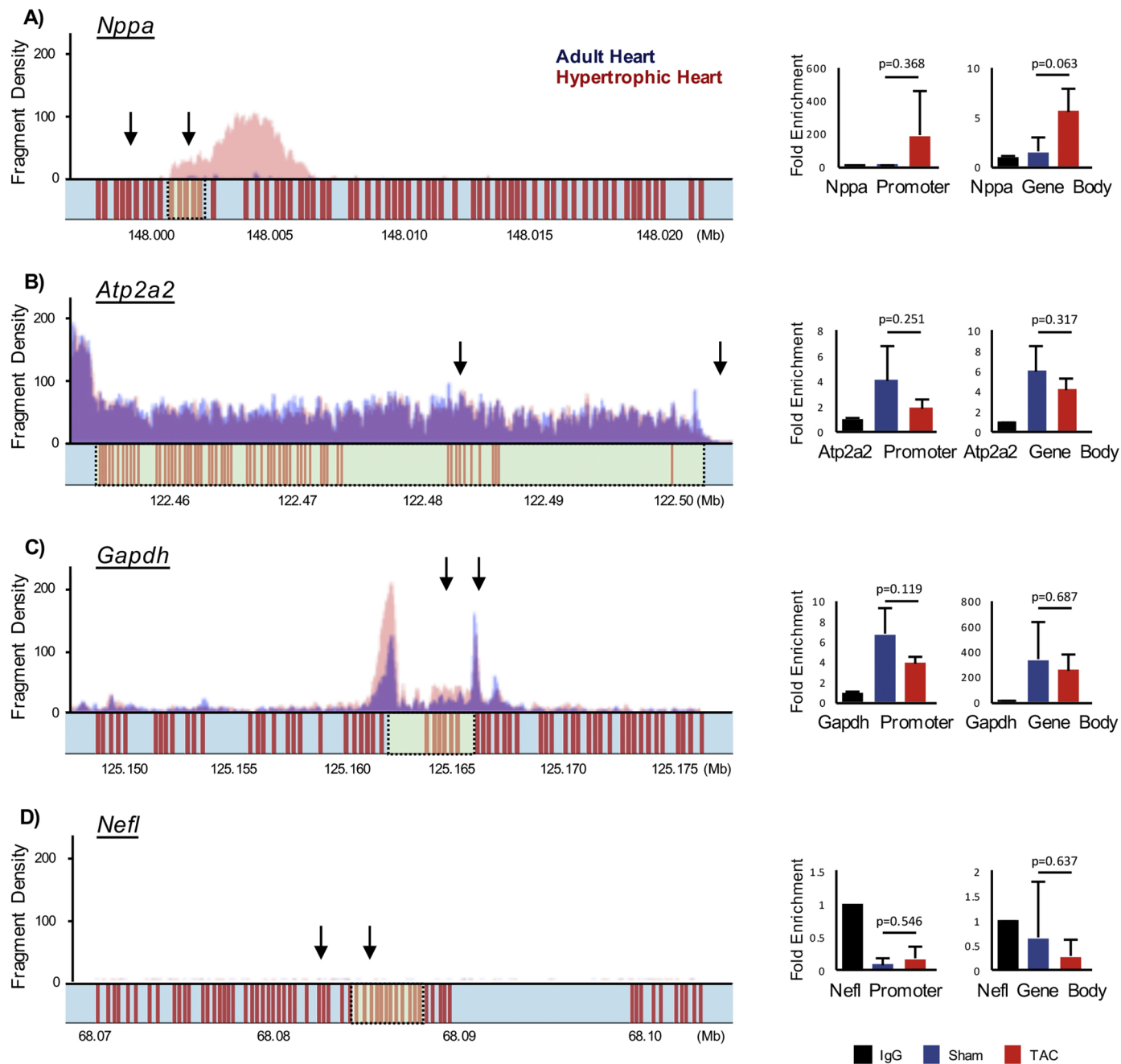


Figure 12